Combining transbronchial biopsy using endobronchial ultrasonography with a guide sheath and positron emission tomography for the diagnosis of small peripheral pulmonary lesions

Hidenori Mizugaki [a], Naofumi Shinagawa [a], Kakuko Kanegae [b], Noriyuki Yamada [a], Hajime Asahina [a], Eiki Kikuchi [a], Satoshi Oizumi [a], Nagara Tamaki [b], Masaharu Nishimura [a]

[a] First Department of Medicine, Hokkaido University School of Medicine, Sapporo 060-8638, Japan

[b] Department of Nuclear Medicine, Hokkaido University Graduate School of Medicine, Sapporo 060-8638, Japan

Correspondence to:

Naofumi Shinagawa, First Department of Medicine, Hokkaido University School of Medicine, North 15, West 7, Kita-ku, Sapporo 060-8638, Japan.

Phone: +81 11 706 5911; Fax: +81 11 706 7899

E-mail address: naofu@med.hokudai.ac.jp

Summary

To evaluate the combination of transbronchial biopsy (TBB) using endobronchial ultrasonography with a guide sheath (EBUS-GS) and positron emission tomography with fluorodeoxyglucose (FDG-PET) for the diagnosis of small peripheral pulmonary lesions (PPLs) ≤30 mm in mean diameter. A total of 74 PPLs (69.2%) were diagnosed by TBB using EBUS-GS with X-ray fluoroscopy. Diagnostic yield by FDG-PET was 78.5% for the 107 PPLs examined. Diagnostic yield with the combination of TBB using EBUS-GS and FDG-PET (90.7%) was significantly higher compared with that for each procedure alone. A significant increment in diagnostic yield with this combination was seen for PPLs >20 mm and ≤30 mm and for malignant lesions. Combination of TBB using EBUS-GS and FDG-PET is useful for the diagnosis of small PPLs.

Key words: peripheral pulmonary lesions; endobronchial ultrasonography with a guide sheath; transbronchial biopsy; positron emission tomography with fluorodeoxyglucose; standardized uptake value

1. Introduction

Various procedures have been developed to diagnose peripheral pulmonary lesions (PPLs). Transbronchial biopsy (TBB) procedures, which use a bronchoscope under fluoroscopic guidance, have been performed since the 1970s, with a diagnostic accuracy of 36-86% [1-5]. This diagnostic accuracy is influenced by lesion size. Schreiber et al. reported in a systematic review that the diagnostic accuracy for lesions <20 mm was 33% [1]. Other studies have found a diagnostic accuracy of 35-50% for benign lesions, lower than that for malignant lesions [2-5].

Currently, small-caliber radial-type ultrasound probes can be used for the clinical application of ultrasonography to examine tracheal-bronchial lesions. Endobronchial ultrasonography (EBUS) has been used for imaging guidance for TBB of PPLs [6,7]. Furthermore, Kurimoto et al. and our own preliminary study have shown the feasibility and effectiveness of TBB using EBUS with a guide sheath (EBUS-GS) [8,9], and several reports have since demonstrated the safety and efficacy of this method [10,11]. Nevertheless, the diagnostic yield of TBB using EBUS-GS in PPLs has been reported as 58-77% [8-13].

Recent advances in positron emission tomography with fluorodeoxyglucose (FDG-PET) have made significant contributions to differentiating between malignant and benign PPLs. Several reports

have suggested that FDG-PET examinations reduce the number of patients with indeterminate PPLs undergoing unnecessary surgical biopsy [14-18]. However, FDG-PET is not always diagnostic, particularly for PPLs ≤30 mm in mean diameter. Malignant lesions such as well-differentiated adenocarcinoma and bronchiolo-alveolar carcinoma are frequently not identified on FDG-PET due to low glucose metabolism, while active inflammation sometimes shows positive FDG uptake due to high glucose metabolism [14-17].

These reports led us to the idea that the combination of TBB using EBUS-GS and FDG-PET might improve diagnostic yields for PPLs. The present study therefore evaluated a combination method for the diagnosis of small PPLs ≤30 mm in diameter.

2. MATERIALS AND METHODS

2.1. Patients

Medical records of 107 patients with 107 small PPLs (mean diameter, ≤30 mm) who underwent both TBB with EBUS-GS and FDG-PET between August 2003 and March 2006 at Hokkaido University Hospital were retrospectively reviewed. PPLs were defined as lesions surrounded by pulmonary parenchyma that were endoscopically

invisible (no evidence of endobronchial lesion, extrinsic compression, submucosal tumor, narrowing, inflammation or bleeding of the bronchus). All chest computed tomography (CT) images were reviewed, and mean diameters of PPLs were recorded. This study was approved by the Internal Review Board at our institution. All patients had provided written informed consent to undergo the procedures described below.

2.2. TBB using EBUS-GS

TBB using EBUS-GS was performed as described previously [8,9]. A 20-MHz mechanical radial-type probe (UM-S20-17R; Olympus Medical Systems, Tokyo, Japan) with an external diameter of 1.4 mm (1.4-mm probe) was most often used, and a 20-MHz mechanical radial-type probe (UM-S20-20R; Olympus) with an external diameter of 1.7 mm (1.7-mm probe) was used for PPLs assumed to be easily reached before bronchoscopy. The probe was connected to an EU-M30S endoscopic ultrasound system (Olympus). A flexible fiberoptic bronchoscope with a 2.0 mm diameter working channel (BF-P-260F; Olympus) and a guide sheath with an external diameter of 1.9 mm (B01-836-12; Olympus) were used for the 1.4-mm probe, and a flexible fiberoptic bronchoscope with a 2.8 mm diameter working channel (BF-1T30 and BF-1T260; Olympus) and a guide sheath with an external diameter of 2.7 mm

(B01-836-13; Olympus) were used for the 1.7-mm probe. After the bronchoscope was inserted under local anesthesia as deeply as possible into the target bronchus under direct vision, an EBUS probe was inserted into the guide sheath, and the guide sheath-covered probe was then inserted through the bronchoscope working channel into the bronchus leading to the area suspected of containing the PPL. EBUS imaging and radiographic fluoroscopy were used to confirm that the probe and guide sheath had reached the PPL. When an EBUS image of the PPL was not obtained, the probe was removed from the guide sheath and a double-hinged curette was inserted into the guide sheath. The appropriate bronchus was then selected by manipulating the curette under fluoroscopic guidance. Once the bronchus was determined, the curette was removed from the guide sheath and the probe was again inserted into the guide sheath to obtain an EBUS image of the PPL. After locating the PPL on the EBUS image, the probe was removed from the guide sheath and the sheath was left in the PPL. Biopsy forceps and bronchial brushes were introduced via the guide sheath, and pathological and cytological specimens were obtained under fluoroscopic guidance. Bronchoscopic procedures were performed by 8 pulmonary fellows, each with >4 years of training and experience in bronchoscopy.

When a definitive diagnosis was not obtained by TBB using

EBUS-GS, the patient underwent other procedures (*e.g.*, video-assisted thoracoscopic surgery (VATS), percutaneous needle biopsy) or clinical and radiological follow-up examinations to confirm diagnosis of the PPL.

2.3. FDG-PET

FDG-PET was performed 60 min after injection of 4.5 MBq/kg body weight of fluorodeoxyglucose using an EXACT 47 scanner (Siemens, Munich, Germany). Patients had to fast for ≥6 h prior to FDG administration. Scanning itself encompassed an emission scan (2 min) and transmission (3 min) using rotating ^{68}Ge-^{68}Ga rod sources. Scans were reconstructed with the ordered subsets expectation maximization algorithm. FDG uptake was evaluated using the maximum standardized uptake value (SUV_{max}). FDG-PET was examined within 4weeks before TBB using EBUS-GS.

2.4. Statistical Analysis

The data that SUV_{max} and diagnostic yields by TBB with EBUS-GS alone and FDG-PET alone were analyzed using Pearson χ^2 test. The diagnostic yields by combining TBB using EBUS-GS and FDG-PET were analyzed using

McNemar test. Statistical software (SPSS version 11.0.1; Chicago, IL) was used for all analyses. Statistical significance was established at the $p < 0.05$ level.

3. RESULTS

3.1. Diagnostic yield by TBB using EBUS-GS

Mean (±standard deviation) diameter of the PPLs was 21.7 ±6.1 mm (range, 9.5-30 mm). Of the 107 PPLs examined, a total of 92 PPLs (86.0%) were detected by EBUS. Definitive diagnosis was established for 74 PPLs (69.2%) by TBB using EBUS-GS (Table 1). Diagnostic yields for PPLs≤20 mm and for PPLs >20 mm and ≤30 mm in mean diameter by TBB using EBUS-GS were 54.5% (24 of 44 PPLs) and 76.2% (48 of 63 PPLs), respectively. The diagnostic yield for PPLs ≤20 mm was significantly lower than that for PPLs >20 mm and ≤30 mm ($p<0.05$). The diagnostic yield tended to be lower for benign disease (50.0%) than for malignant disease (72.5%), but this difference was not statistically significant.

3.2. Diagnostic yield by FDG-PET

In all PPLs, mean SUV_{max} for FDG-PET was 4.2 ±2.9. A significant difference in SUV_{max} was seen between malignant disease (4.5 ±3.0) and benign disease (2.5 ±1.6; $p<0.01$). With malignant disease, a significant difference in SUV_{max} was seen between PPLs ≤20 mm (2.9 ±1.4) and PPLs >20 mm and ≤30 mm (5.5 ±3.2; $p<0.01$). Conversely, with benign disease, no significant differences were seen according to tumor size (Table 2).

To determine a cut-off value of SUV_{max} for diagnosing pulmonary malignancy with FDG-PET, we analyzed the receiver operating characteristics (ROC) curve of SUV_{max} in all PPLs. The ROC curve showed that a cut-off value of 2.0 would provide the highest sensitivity and specificity (Fig. 1). We then selected a cut-off value of 2.0 of SUV_{max} for the following analysis in this study.

When using this criterion, diagnostic yield was 78.5% for the 107 PPLs examined. Diagnostic yields by FDG-PET of PPLs ≤20 mm and PPLs >20 mm and ≤30 mm were 70.5% (31 of 44 PPLs) and 84.1% (53 of 63 PPLs), respectively. Diagnostic yield was significantly lower for PPLs≤20 mm than for PPLs >20 mm and ≤30 mm ($p<0.01$). Diagnostic yield was also significantly lower for benign disease (56.3%) than for malignant disease (82.4%; $p<0.01$).

3.3. Diagnostic yield with combination of TBB using EBUS-GS and

FDG-PET

Next, the diagnostic yield by combining TBB using EBUS-GS and FDG-PET was evaluated (Table 3; results for each method are also shown). Diagnostic yield with the combination of TBB using EBUS-GS and FDG-PET was 90.7% for the 107 PPLs examined. In addition, sensitivity, specificity, positive predictive value, and negative predictive value for combination of TBB using EBUS-GS and FDG-PET were 94.5%, 68.8%, 94.5%, and 68.8%, respectively. According to size, diagnostic yield for PPLs >20 mm and ≤30 mm in mean diameter reached 96.8%, while diagnostic yield for PPLs ≤20 mm was 81.8%. When restricted to malignant diseases, diagnostic yield with the combination of techniques (94.5%) was still significantly higher than those for each procedure alone (72.5% by TBB with EBUS-GS alone; 82.4% by FDG-PET alone). Diagnostic yield for malignant diseases with PPLs >20 mm and ≤30 mm using the combination method reached 100%. Conversely, no significant differences in diagnostic yields were seen for benign disease, although diagnostic yield with the combination method (68.8%) tended to be higher than those for each procedure alone (50.0% for EBUS-GS alone; 56.3% for FDG-PET alone).

3.4. Non-diagnostic lesions by both TBB using EBUS-GS and

FDG-PET

Even after combining TBB using EBUS-GS with FDG-PET, diagnostic yields did not reach 100%, and 10 PPLs were not diagnosed even by the combination method. These 10 PPLs comprised 5 malignant lesions (adenocarcinoma, n=3; large cell carcinoma, n=1; metastasis of renal cell carcinoma, n=1) and 5 benign lesions (pneumonia, n=3; radiation pneumonitis, n=1; and pneumoconiosis, n=1). Six PPLs (5 malignant lesions and 1 pneumoconiosis lesion) were diagnosed by VATS, 1 PPL (radiation pneumonia) by repeated TBB using EBUS-GS, and 3 PPLs (pneumonia) by follow-up examinations. Mean diameter of these PPLs was 16.4 mm. Mean SUV_{max} for the 5 malignant PPLs and 5 benign PPLs were 1.39 and 3.53, respectively.

3.5. Representative cases

The first case involved a 61-year-old man presenting with a small PPL 10 mm in mean diameter in the left segment 4 (Fig. 2). On FDG-PET, slight FDG uptake was observed in the left upper lobe (SUV_{max}, 1.45). The PPL was diagnosed as lung adenocarcinoma. This case was representative of a false-negative finding on FDG-PET.

The second case involved a 74-year-old man with chronic obstructive

pulmonary disease (COPD) presenting with a small PPL of 15 mm in mean diameter in segment 6 of the right lung (Fig. 3). On FDG-PET, high uptake was seen in the right lower lobe (SUV_{max}, 4.52). TBB using EBUS-GS was not diagnostic, while partial resection by VATS revealed squamous cell carcinoma. This case was representative of cases in which FDG-PET was useful for the diagnosis of malignant disease, but TBB with EBUS-GS was not.

4. DISCUSSION

The present study combined TBB using EBUS-GS with FDG-PET for the diagnosis of small PPLs ≤30 mm in mean diameter. This is the first report that shows the usefulness of combination of EBUS-GS and FDG-PET for pulmonary peripheral lesions. As a result, diagnostic yield with this combination was >90%, significantly higher than with each procedure alone. We have provided novel, important evidence that the combination of TBB using EBUS-GS and FDG-PET is useful in the diagnosis of small PPLs. Chhajed et al. have already reported the usefulness of combining TBB with FDG-PET in the diagnosis of small PPLs≤30 mm in mean diameter [19]. However, they used conventional bronchoscopy, and the diagnostic yield of bronchoscopy was 53%, including 8% for endobronchial lesions. As TBB with EBUS-GS is

obviously superior to conventional bronchoscopy, particularly for the diagnosis of smaller PPLs [8-13], our results will contribute to the development of diagnostic procedures for small PPLs.

Some previous reports have used a cut-off SUV_{max} of 2.5 [15,19], but no obvious validation has been provided for this value, particularly for small PPLs ≤ 30 mm in mean diameter. In the present study, we selected a cut-off SUV_{max} of 2.0, as the ROC curve of SUV_{max} for all PPLs showed that this value offered higher sensitivity and specificity than 2.5. Bryant et al. reported that in small PPLs ≤ 25 mm, 24% of nodules with SUV_{max} ≤2.5 were malignant [20]. When using a cut-off of 2.0, diagnostic yield by FDG-PET was 78.5% for the 107 PPLs examined (82.4% for malignant, 56.3% for benign), similar to the findings of previous studies [21]. Determining the optimal cut-off value for FDG-PET in each study using reliable methods such as ROC curves is important.

However, FDG-PET is not always diagnostic, particularly for small PPLs. Small malignant lesions ≤ 30 mm in mean diameter could show lower FDG uptake than larger malignant tumors, due to partial-volume effects [22]. Malignant lesions such as well-differentiated adenocarcinoma and bronchiolo-alveolar carcinoma are frequently missed by FDG-PET due to low glucose metabolism [12-15,17,18]. In this study, the 44 adenocarcinomas included 14 PPLs that were false-negative on FDG-PET, and pathological review showed that these

14 PPLs comprised 11 well-differentiated adenocarcinomas and 3 bronchiolo-alveolar carcinomas. Of note is the fact that the 11 adenocarcinomas were successfully diagnosed by TBB using EBUS-GS, even without positive FDG-PET findings.

In contrast, there are false-positives in FDG-PET for detecting pulmonary malignancy. Physicians always have to consider the possibility that FDG-PET findings are false-positive as malignant lesions, especially in pulmonary benign diseases such as sarcoidosis or active inflammatory changes. In the case, again, EBU-GS is useful; definitive identification can be accomplished by TBB with EBUS-GS, referring to clinical features or laboratory data. Subsequently, patients are able to receive proper treatment.

Even after combining TBB using EBUS-GS with FDG-PET, diagnostic yield did not reach 100%. The increment in diagnostic yield with the combination method was more apparent with PPLs >20 mm and ≤30 mm and with malignant lesions. Ten PPLs remained undiagnosed even with the combination method. These 10 PPLs comprised 5 malignant lesions and 5 benign lesions, and mean diameter of these PPLs was 16.4 mm. The limitations of the combination method must be kept in mind, particularly in small PPLs ≤20 mm. The present study encountered no complications associated with TBB using EBUS-GS or FDG-PET that required hospitalization.

5. Conclusion

In conclusion, based on our retrospective analysis, the combination of TBB with EBUS-GS and FDG-PET increased diagnostic yield to >90%, representing a useful method for the diagnosis of small PPLs ≤30 mm. In cases where neither TBB using EBUS-GS nor FDG-PET is diagnostic, the combination strategy supports the decision of the physician as to whether more invasive procedures or clinical and radiological follow-up are required for the management of PPLs.

Acknowledgements

We gratefully acknowledge the outstanding support of Dr. Koichi Yamazaki, former Associate Professor of the First Department of Medicine at Hokkaido University School of Medicine.

Conflict of Interest statement

The authors have no conflict of interest to declare.

REFERENCES

[1] Schreiber G, McCrory DC. Performance characteristics of different modalities for diagnosis of suspected lung cancer: summary of published evidence. Chest 2003; 123:115s-128s

[2] Baaklini WA, Reinoso MA, Gorin AB, et al. Diagnostic yield of fiberoptic bronchoscopy in evaluating solitary pulmonary nodules. Chest 2000; 117:1049-1054

[3] Chechani V. Bronchoscopic diagnosis of solitary pulmonary nodules and lung masses in the absence of endobronchial abnormality. Chest 1996; 109:620-625

[4] Gasparini S, Ferretti M, Secchi EB, et al. Integration of transbronchial and percutaneous approach in the diagnosis of peripheral pulmonary nodules or masses: experience with 1,027 consecutive cases. Chest 1995; 108:131-137

[5] Radke JR, Conway WA, Eyler WR, et al. Diagnostic accuracy in peripheral lung lesions. Factors predicting success with flexible fiberoptic bronchoscopy. Chest 1979; 76:176-179

[6] Herth FJF, Ernst A, Becker HD, et al. Endobronchial ultrasound-guided transbronchial lung biopsy in solitary pulmonary nodules and peripheral lesions. Eur Respir J 2002; 20:972-974

[7] Paone G, Nicastri E, Lucantoni G, et al. Endobronchial ultrasound-driven biopsy in the diagnosis of peripheral lung lesions. Chest 2005;

128:3551-3557

[8] Kurimoto N, Miyazawa T, Okimasa S, et al. Endobronchial ultrasonography using a guide sheath increases the ability to diagnose peripheral pulmonary lesions endoscopically. Chest 2004; 126:959-965

[9] Kikuchi E, Yamazaki K, Sukoh N, et al. Endobronchial ultrasonography with guide-sheath for peripheral pulmonary lesions. Eur Respir J 2004; 24:533-537

[10] Shirakawa T, Imamura F, Hamamoto J, et al. Usefulness of endobronchial ultrasonography for transbronchial lung biopsies of peripheral lung lesions. Respiration 2004; 71:260-268

[11] Herth FJF, Eberhardt R, Becker HD, et al. Endobronchial ultrasound-guided transbronchial lung biopsy in fluoroscopically invisible solitary pulmonary nodules: prospective trial. Chest 2006; 129:147-150

[12] Asahina H, Yamazaki K, Onodera Y, et al. Transbronchial biopsy using endobronchial ultrasonography with a guide sheath and virtual bronchoscopic navigation. Chest 2005; 128:1761-1765

[13] Yamada N, Yamazaki K, Kurimoto N, et al. Factors related to diagnostic yield of transbronchial biopsy using endobronchial ultrasonography with a guide sheath in small peripheral pulmonary lesions. Chest 2007; 132:603-608

[14] Scott WJ, Schwabe JL, Gupta NC, et al. Positron emission tomography of lung tumors and mediastinal lymph nodes using [^{18}F] fluorodeoxyglucose. Ann. Thorac. Surg. 1994; 58:698–703.

[15] Patz EF, Lowe VJ, Hoffman JM, et al. Focal pulmonary abnormalities: evaluation with F-18 fluorodeoxyglucose PET scanning. Radiology. 1993; 188:487–490.

[16] Gupta NC, Maloof J and Gunel E. Probability of malignancy in solitary pulmonary nodules using fluorine-18-FDG and PET. J Nucl Med. 1996; 37:943–948.

[17] Gupta NC, Gill H, Graeber G, et al. Dynamic positron emission tomography with F-18 fluorodeoxyglucose imaging in differentiation of benign from malignant lung/mediastinal lesions. Chest 1998; 114: 1105–1111.

[18] Gambhir SS, Shepherd JE, Shah BD, et al. Analytical decision model for the cost-effectiveness management of solitary pulmonary nodules. J Clin Oncol. 1998; 16:2113–2125.

[19] Chhajed PN, Bernasconi M, Gambazzi F, et al. Combining bronchoscopy and positron emission tomography for the diagnosis of the small pulmonary nodule < or = 3 cm. Chest 2005; 128:3558-3564

[20] Bryant AS, Cerfolio RJ. The maximum standardized uptake values on integrated FDG-PET/CT is useful in differentiating benign from

malignant pulmonary nodules. Ann Thorac Surg. 2006; 82:1016–1020

[21] Farrell MA, McAdams HP, Herndorn JE, et al. Non-small cell lung cancer: FDG PET for nodal staging in patients with stage Ⅰ disease. Radiology. 2000; 215:886-890

[22] Key JW Jr. SUV : Standerd uptake or silly useless value? J Nucl Med. 1995; 36:1836-1839

FIGURE LEGENDS

Figure 1: Receiver operating characteristics (ROC) curve of SUV_{max} in all PPLs. The ROC curve showed that the cut-off value of 2.0 offered the highest sensitivity and specificity.

Figure 2: Images from a 61-year-old man with lung adenocarcinoma showing false-negative findings on FDG-PET. **A)** On chest CT, a small PPL 10 mm in mean diameter is seen in segment 4 of the left lung. **B)** EBUS revealing the PPL, which was diagnosed as adenocarcinoma by TBB using EBUS-GS. **C, D)** On FDG-PET, transverse and coronal scans demonstrate slight FDG uptake in the left upper lobe (SUV_{max}, 1.45).

Figure 3: Images from a 74-year-old man with COPD and squamous cell carcinoma of the lung showing positive findings on FDG-PET. **A)** On chest CT, a small PPL 15 mm in mean diameter is seen in segment 6 of the right lung. **B)** On FDG-PET, coronal scan demonstrates higher FDG uptake in the right lower lobe (SUV_{max}, 4.52).

Table 1: Established diagnosis in all 107 lesions

Diagnosis	Lesions diagnosed by TBB using EBUS-GS / total lesions
Malignant	66 / 91
Lung cancer	59 / 80
Adenocarcinoma	33 / 44
Squamous cell carcinoma	12 / 17
Large cell carcinoma	1 / 4
Non-small cell carcinoma	6 / 7
Small cell carcinoma	7 / 8
Metastatic lung tumor	5 / 9
Lymphoma	1 / 1
Sarcoma	1 / 1
Benign	8 / 16
Non-tuberculous mycobacteriosis	3 / 4
Tuberculosis	1 / 1
Organizing pneumonia	2 / 2
Inflammatory change	0 / 4
Lung abscess	2 / 2
Others	0 / 3

Table 2: Mean maximum standard uptake for FDG-PET

	≤20 mm	>20 mm and ≤30 mm	Total
Malignant	2.9 ± 1.4	5.5 ± 3.2	4.5 ± 3.0
Benign	2.5 ± 1.6	2.5 ± 1.8	2.5 ± 1.6
Total	2.8 ± 1.5	5.2 ± 3.2	4.2 ± 2.9

Values represent mean ± standard deviation.

Table 3: Diagnostic yields of combination TBB using EBUS-GS and FDG-PET

	≤ 20mm			>20 mm and ≤30 mm			Total		
	EBUS-GS	FDG-PET	EBUS-GS/ FDG-PET	EBUS-GS	FDG-PET	EBUS-GS/ FDG-PET	EBUS-GS	FDG-PET	EBUS-GS/ FDG-PET
Malignant	57.1%	74.3%	85.7%* (n = 35)	78.6%	87.5%	100%† (n = 56)	72.5%	82.4%	94.5%‡ (n = 91)
Benign	44.4%	55.6%	66.7% (n = 9)	57.1%	57.1%	71.4% (n = 7)	50.0%	56.3%	68.8% (n = 16)
Total	54.5%	70.5%	81.8%* (n = 44)	76.2%	84.1%	96.8%† (n = 63)	69.2%	78.5%	90.7%‡ (n = 107)

*$p < 0.01$ compared to EBUS-GS

†$p < 0.01$ compared to EBUS-GS and $p < 0.05$ compared to FDG-PET

‡$p < 0.01$ compared to EBUS-GS and FDG-PET

Date were analyzed using the McNemar test

Figure 1

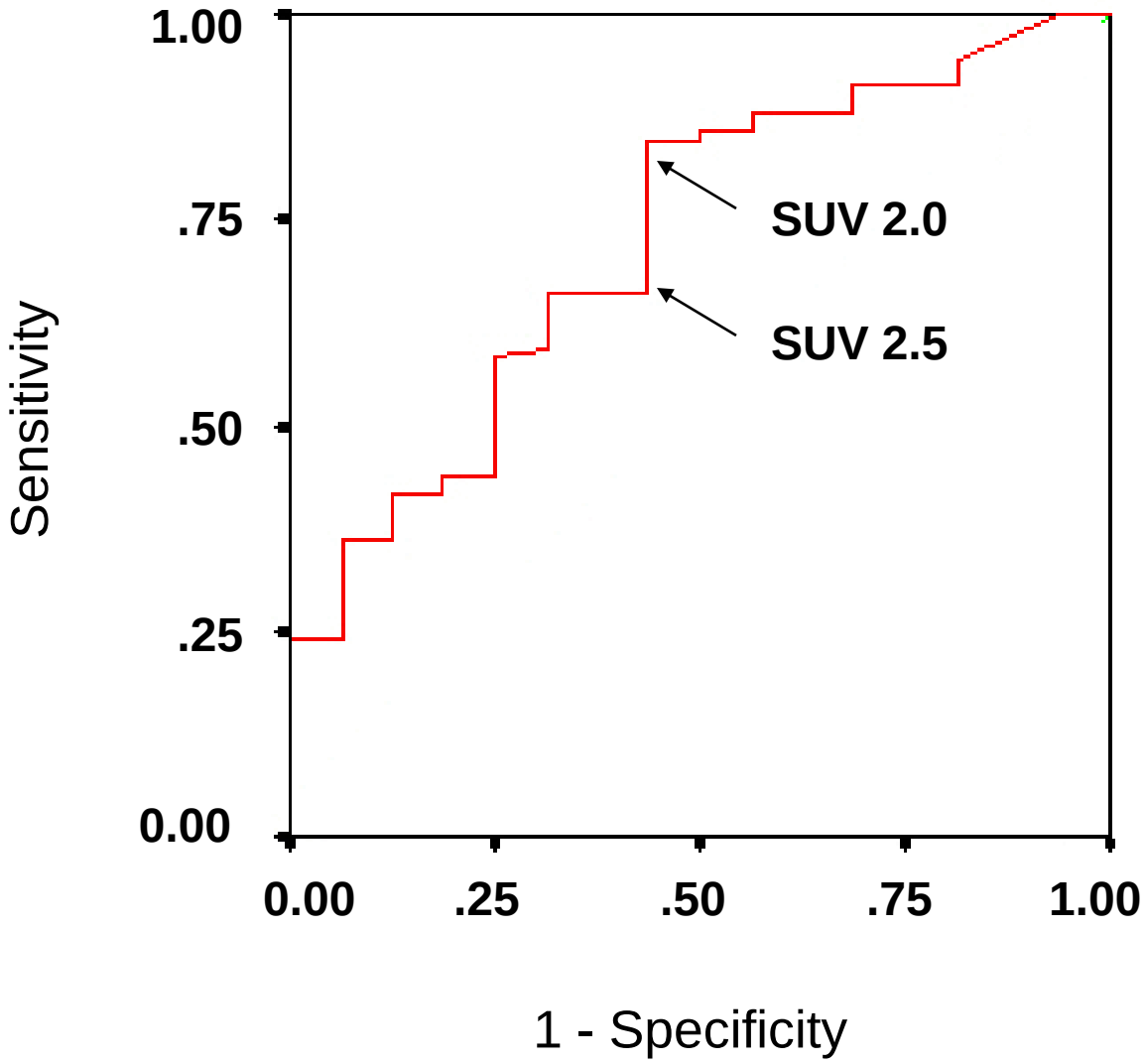
1.00
.75
.50
.25
0.00
Sensitivity
SUV 2.0
SUV 2.5
0.00
.25
.50
.75
1.00
1 - Specificity

Figure 2

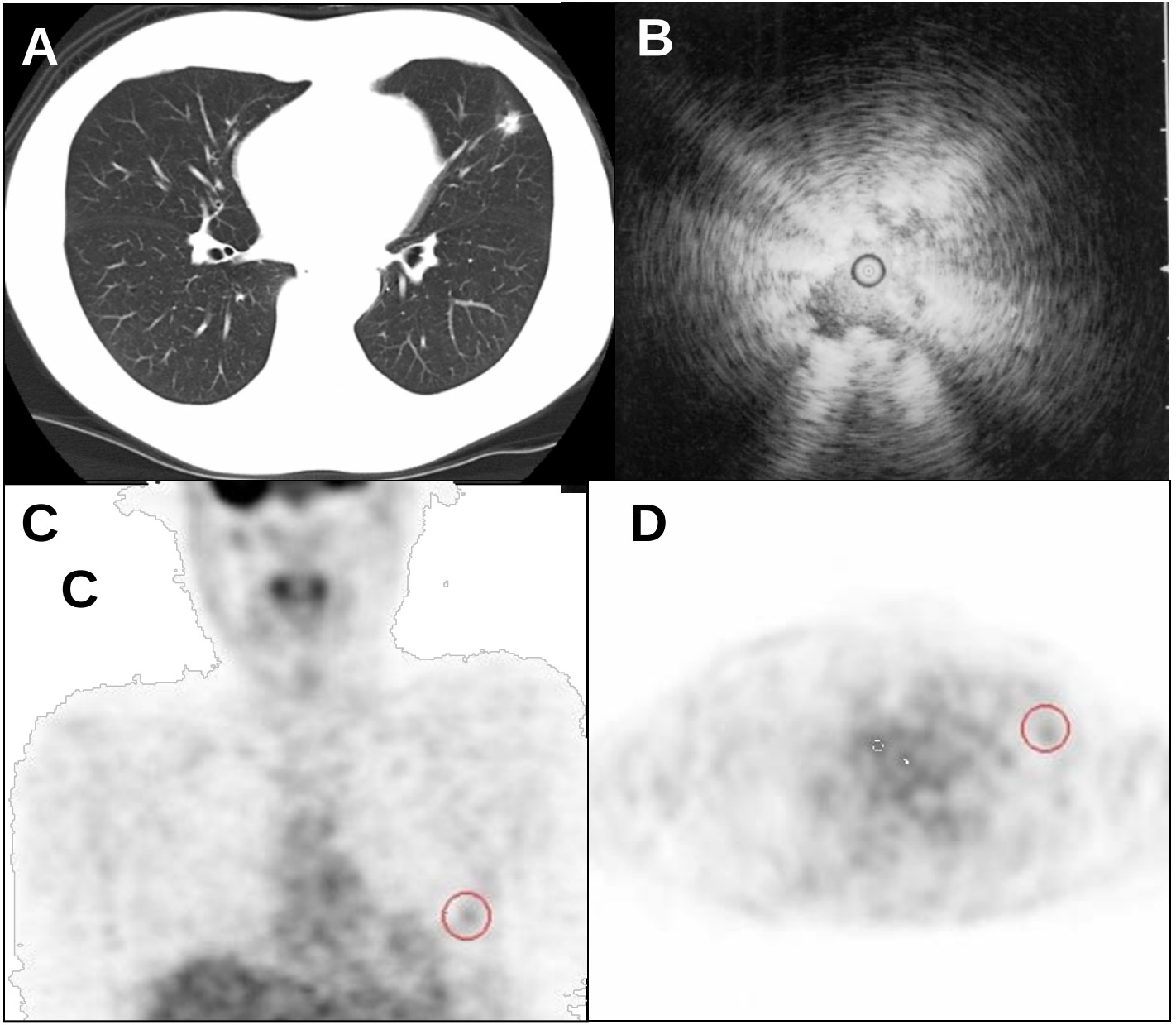

Figure 3